

Frequency-Locked Motion of Two Particles in a Paul Trap

J. Hoffnagle and R. G. Brewer

IBM Almaden Research Center, 650 Harry Road, San Jose, California 95120

(Received 19 May 1993)

The nonlinear dynamics of two ions in a Paul trap is known to show chaos or condensation into a regular "crystal." We present the first observations of frequency locking of two microspheres (diameter $10\ \mu\text{m}$) in a Paul trap, in close agreement with theoretical predictions. This system reproduces the main features of our earlier work on two-ion chaos. The phase space is fragmented, and chaotic transients can converge to several regular attractors. Damping, including laser cooling, can extinguish frequency-locked attractors, explaining their absence in ion trap experiments. Study of coupled circle maps shows that this is a general phenomenon when three frequencies are present.

PACS numbers: 05.45.+b, 03.20.+i, 32.80.Pj, 52.55.Mg

Laser cooling of trapped ions can produce ionic *Coulomb clusters*, in which the electrostatic energy is comparable to or larger than the thermal kinetic energy [1, 2]. The lowest energy configurations have been called "ion crystals" and are easily understood as equilibria between the time-averaged confining force of the trap and the electrostatic repulsion of the ions. There is also a phenomenon resembling melting: As the trapping parameters are varied an abrupt transition occurs between the crystal and a diffuse, extended state of motion. We have interpreted this transition, for the particular case of two ions in a Paul trap, as being between order and deterministic chaos [3]. Further understanding of the dynamics came with the realization that the orbits can evolve on long time scales before transient chaos reduces to regular motion. At a critical value of the control parameter transient chaos gives way to stationary chaos [4].

The simplest cluster is a very elementary nonlinear system: two classical particles in a periodic trap potential, interacting by the Coulomb force. Their motion ideally follows coupled Mathieu-Coulomb equations, discussed below, which have both regular and chaotic solutions, depending on initial conditions. The crystal is the best known regular solution, but calculations also reveal an extensive family of frequency-locked orbits [3, 5], closed orbits with a period that is a multiple of that of the trap potential. Frequency locking is prevalent in periodically forced systems when a nonlinearity pulls the natural frequencies into a rational relation [6]. Clearly the periodic orbits are essential to an understanding of the dynamics, so it is puzzling that frequency-locked motion has not been found in ion trap experiments [1, 3, 4, 7]. Here we report the first observation of two-particle frequency locking, as predicted by our calculations.

Apparatus.—The "melting" and "freezing" of Coulomb clusters was observed over thirty years ago, in one of the first demonstrations of electrodynamic trapping [8]. We have designed a similar apparatus using a Paul trap with hyperboloidal electrodes (ring radius $r_0 = 1\ \text{cm}$) to confine polymer beads ("microspheres") of about $10\ \mu\text{m}$ diameter, charged to $5\text{--}10\ \mu\text{C/g}$. Access to the center of

the trap, for particle loading, illumination, and viewing, is through holes of 3 mm radius on the axis of the end caps and in four places around the ring. The holes in the end caps were covered with $0.127\ \text{mm}$ pitch Ni mesh to minimize the distortion of the trapping field. Covering the ring with mesh degraded the images of the particles unacceptably, so these holes were left open. The trap and particle source were enclosed in a rough vacuum of $1.5\ \text{Pa}$ to reduce aerodynamic drag. The trap was used as a filter to select particles with equal charge-to-mass ratio and a constant potential applied between the end caps to balance gravity. The beam from a semiconductor laser was collimated to $4.5\ \text{mm}$ diameter, circularized, and directed through the ring electrode, and the light scattered at right angles was recorded with a video camera. By modulating the laser current, the illumination could be pulsed synchronously with the trap voltage, giving a set of stationary points when frequency locking occurs.

The Paul trap with microspheres has two major advantages for the study of the basic nonlinear dynamics of Coulomb clusters. Since the equations of motion ideally depend only on dimensionless combinations of charge and mass, the dynamics is essentially the same for particles of *any* size. The physical time and length scales of an experiment do depend on size, however, leading to a fundamental problem when studying trapped ions: the inability to observe trajectories on the natural dynamical time scale, due to the limited photon scattering rate. Microspheres scatter more light than single ions, and because of their smaller charge-to-mass ratio the trap operates at $\sim 100\ \text{Hz}$ rather than MHz. It is thus relatively easy to track the particle motion on the time scale of the trap frequency. Damping is important in practical particle traps, and in this respect, too, replacing ions with larger particles is advantageous. Ions are cooled by radiation pressure [9] which has a highly nonlinear velocity dependence. This additional nonlinearity obscures and can even overshadow the Coulomb interaction we wish to study [7, 10]. It may lead to nontrivial dynamics for only a single trapped ion [11]. Moreover, the random nature of photon emission and absorption gives a stochastic

component to the light pressure force [12–14]. The aerodynamic drag on microspheres is proportional to velocity and represents a minor modification to the equations of motion. The principal drawback of microspheres is that they are not precisely identical, as ions are. Even though the trap can be used as a filter to select particles with the same charge-to-mass *ratio*, some dispersion in size is unavoidable. Fortunately this does not seem to qualitatively affect the motion, provided the mass discrepancy is not too large.

Equations of motion.—We briefly review the operation of an ideal Paul trap, defined by an oscillatory, quadrupole potential,

$$V(\mathbf{r}) = (V_{\text{dc}} - V_{\text{ac}} \cos \Omega t) \frac{x^2 + y^2 - 2z^2}{2r_0^2}. \quad (1)$$

The motion of a particle of charge e and mass m can be expressed in dimensionless form by introducing a new time variable, $\tau = \Omega t/2$, and dimensionless potentials,

$$a_1 = a_2 = \frac{4eV_{\text{dc}}}{mr_0^2\Omega^2}, \quad a_3 = -2a_1, \quad (2)$$

$$q_1 = q_2 = \frac{2eV_{\text{ac}}}{mr_0^2\Omega^2}, \quad q_3 = -2q_1. \quad (3)$$

The equations of motion for a single particle separate into independent Mathieu equations for each Cartesian component. For $a_i = 0$ stable single-particle motion is possible in the parameter range $0 < q_3 < q_M$, where q_M is numerically determined to have the value $q_M = 0.908046\dots$. The bounded Mathieu functions have a Floquet series expansion [15] which may be interpreted as harmonic oscillations at the secular frequencies $\omega_i = \frac{1}{2}\beta_i(a_i, q_i)\Omega$ modulated by “micromotion” with frequency Ω .

For two identical particles the motion separates into a center-of-mass component, obeying linear Mathieu equations, and a relative component, which has a nonlinear contribution from the Coulomb force. Denoting the relative coordinate by \mathbf{r} and introducing a natural unit of length, $[\ell] = (2e^2/m\Omega^2)^{1/3}$, one obtains the equations of motion for the Cartesian components r_i :

$$\ddot{r}_i + \Gamma \dot{r}_i + (a_i - 2q_i \cos 2\tau - |\mathbf{r}|^{-3})r_i = 0. \quad (4)$$

Here dots denote differentiation with respect to τ and the term in Γ describes linear damping due to Stokes’s law. In this system (the *Mathieu-Coulomb equations*) the three components are coupled by the Coulomb term $r_i/|\mathbf{r}|^3$. Many calculations have been done with the simplified system having only one radial coordinate, which shows essentially the same behavior as the three-dimensional equations.

Equation (4) was investigated by numerical integration, using the Bulirsch-Stoer algorithm of Ref. [16], with parameters matching the experiments: $a_i = 0$ and $\Gamma = 10^{-2}$. The trap then has a single parameter, q_3 ,

henceforth abbreviated q . In the crystal the particles lie in the $z = 0$ plane, oscillating at frequency Ω about their average positions. Other stable states were found by integrating the equations of motion starting with random initial conditions corresponding to large total energy; the ensuing chaotic transient evolves to a stable attractor, either the crystal or a periodic orbit. Although this method of finding periodic orbits requires some dissipation, the orbits themselves correspond to periodic solutions of the underlying Hamiltonian problem, as was verified by gradually reducing Γ to zero. (These numerical experiments were carried out with the interactive program “DYNAMICS” [17].) Simulations with $\Gamma = 10^{-3}$ showed additional frequency-locked solutions, stable over narrow ranges of q , which disappeared when Γ was raised, indicating that although dissipation is an experimental necessity and computationally useful, it tends to *destabilize* the periodic orbits.

Other perturbations may also destabilize the periodic orbits. We have investigated this by modifying Eq. (4), focusing in particular around $q = 0.73$, where there are two prominent attractors, with periods 4 and 8. An especially important perturbation is the nonlinearity due to the average light pressure force. When it is added to the Mathieu-Coulomb equations, the only regular solutions are the crystal and the period-4 orbit. It thus appears that laser cooling may represent a serious obstacle to observing frequency locking in ion traps.

Results.—Experimentally, frequency-locked states were prepared from the two-particle crystal by raising q to near the stability limit q_M , where perturbations displace the particles enough to initiate chaotic motion. If q is then reduced to a value for which periodic motion is stable, the chaotic transient can be attracted to this orbit or to the crystalline state. In this way we have observed four periodic orbits in the region $0.65 < q < 0.80$. Pictures of the trajectories, taken with continuous illumination, are reproduced in the left-hand column of Fig. 1 and the corresponding calculated orbits are plotted on the right. They are labeled by their winding numbers, w_r and w_z , the rational ratios of the secular to trap frequencies. With the exception of the period-4 orbit, the winding numbers approximate $\beta_r/2$ and $\beta_z/2$, i.e., the secular frequencies relative to Ω of a single, undamped particle at the same value of q . In comparing the observed and calculated trajectories in Fig. 1 several considerations should be borne in mind: (1) The right-hand column of Fig. 1 shows solutions of Eq. (4) for the *relative coordinate* of the particles. The observations on the left show the full coordinates of both particles. Since the center of mass is at rest at the trap origin, the computed trajectories in full spatial coordinates would look like the relative coordinate augmented by its reflection in the origin. (2) The computed trajectories are plotted in radial and axial coordinates. Actually, the radial motion can lie in any plane that includes the z axis; in general this

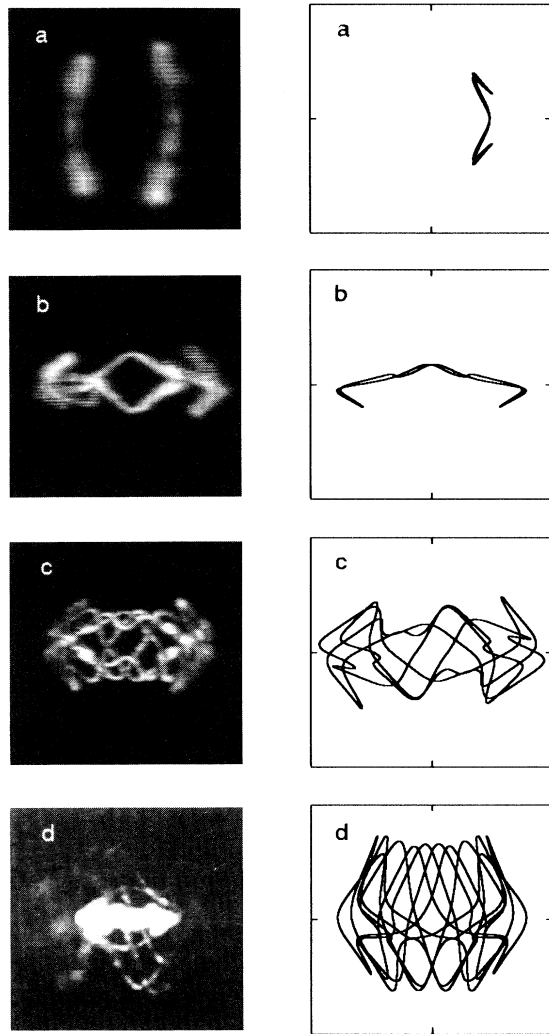


FIG. 1. Frequency-locked two-particle Coulomb clusters. Left column: photographs taken with cw illumination. Right column: computed trajectories of the relative coordinate (r, z) of the two particles for the same q values and $\Gamma = 10^{-2}$. The values of q and winding numbers (w_r, w_z) are (a): $q = 0.72$, $(4/4, 1/4)$; (b): $q = 0.74$, $(1/8, 2/8)$; (c): $q = 0.78$, $(3/22, 7/22)$; and (d): $q = 0.79$, $(5/36, 12/36)$. The mass ratio of the particles is approximately 1 in (a)–(c) and 1.25 in (d).

is not perpendicular to the viewing direction and the radial motion appears foreshortened. In Fig. 1(c) one also sees blurring of the edges of the trajectory, due to the limited depth of focus of the optics. For the period-4 orbit, Fig. 1(a), it was ascertained by looking through the top end cap that the motion was at approximately 45° to the direction of view. When the resulting foreshortening is taken into account, the shape of the observed orbit is in good quantitative agreement with the calculation. (3) Figure 1(d) also suffers from the limited diameter of the illuminating laser beam, resulting in a poor image over

TABLE I. Experimental and theoretical stability ranges for frequency locking.

Winding numbers (w_r, w_z)	Range of q	
	Observed	Calculated
$(4/4, 1/4)$	$<0.67 - 0.762^a$	$0.643 - 0.762$
$(1/8, 2/8)$	$<0.72 - 0.783^a$	$0.698 - 0.763$
$(3/22, 7/22)$	$0.779 - 0.796$	$0.765 - 0.790$
$(5/36, 12/36)$	$0.784 - 0.792$	$0.789 - 0.792$

^aLower limit was not established experimentally because of the large extension of the orbits at low q . See the text for further discussion.

much of the motion.

Under stroboscopic illumination, a stationary pattern of points is observed, as expected for periodic motion. For the period-4 and -8 orbits, it is possible to verify the periodicity by counting the number of points per orbit. The images of the higher-period orbits are too cluttered to resolve all the points, especially since they often overlap along the line of sight, but it is still significant that the patterns are stationary.

Once the frequency-locked motion was established, the trapping voltage was slowly varied to determine the range of q over which the orbit is stable. The results are compared with numerical solutions of Eq. (4) in Table I and Fig. 2. For low q the period-4 and -8 orbits become comparable in size to the trap itself, preventing an experimental determination of the lower end points of their stability ranges. The agreement between theory and experiment gives us confidence in the assignment of winding numbers. Not only do the calculations reproduce the observed frequency-locked states, with one exception they give *only* the observed states. The single unobserved, calculated solution in the range of Fig. 2 had winding numbers $(3/24, 7/24)$ and existed for $0.730 < q < 0.735$. It was sensitive to damping, disappearing at $\Gamma = 2 \times 10^{-2}$,

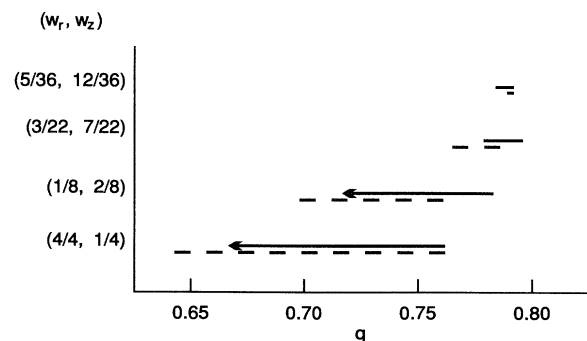


FIG. 2. Stability of periodic motion. The observed (solid) and computed (dashed) ranges of stability are plotted for the four observed periodic orbits, labeled by their winding numbers. The arrows signify that the lower limits of the period-4 and -8 orbits could not be reached experimentally, as discussed in the text.

and was probably only barely stable under our experimental conditions.

We have thus shown that the possibilities for regular motion in Coulomb clusters are much richer than crystallization alone: rather the nonlinear interaction can lead to frequency locking in a large family of stable, periodic orbits. For some parameter values there are several coexisting attractors, leading to multistability in a fragmented phase space. The agreement between our observations and calculations supports the point of view that the essential features of Coulomb cluster dynamics are described by the Mathieu-Coulomb equations.

Our observations were performed in an apparatus with considerable dissipation, but calculations indicate that this is not necessary for frequency locking, since the periodic solutions have their origin in the Hamiltonian equations of motion underlying the dynamics of all Coulomb clusters. With reduced damping even more frequency-locked states appear, though they may be sensitive to perturbations. A numerical calculation with $\Gamma = 10^{-3}$ found 28 stable orbits with periods under 100 trap periods in the range $0.7 < q < q_M$, and it is likely that this count is incomplete. Even though they may be destabilized by damping or other perturbations, the existence of these solutions suggests that chaos in ion traps is organized around multistable, periodic motion.

We expect that similar frequency-locking phenomena are a general feature of systems with three or more frequencies. Since circle maps have a wide applicability in modeling physical systems [18], we have considered a simple model of two coupled circle maps. This has the essential features of two nonlinearly coupled incommensurate frequencies with a common driving frequency. For some choices of the parameters we find behavior similar to the solutions of Eq. (4): regions where the winding numbers are rational, with common denominators, interspersed with zones of irrational winding numbers. Multiple periodic orbits also appear for some parameters. The model allows more rapid calculations than numerical integration of differential equations, so it could be more suitable for investigating universality in multidimensional frequency locking.

Finally, we speculate on the possibility of observing frequency-locked, laser-cooled, trapped ions. Calculations indicate that the large nonlinearity associated with

the cooling presents a serious obstacle, but the parameter space of laser detuning and Rabi frequency has not been thoroughly explored. Further experiments and calculations will be required to clarify this point.

Debra Fenzel-Alexander provided the polymer sample with which most experiments were done. The assistance of Ken Foster in constructing the apparatus and discussions with Mark Seymour on the triboelectric charging of polymers are also gratefully acknowledged.

-
- [1] F. Diedrich, E. Peik, J. M. Chen, W. Quint, and H. Walther, *Phys. Rev. Lett.* **59**, 2931 (1987).
 - [2] D. J. Wineland, J. C. Bergquist, W. M. Itano, J. J. Bollinger, and C. H. Manning, *Phys. Rev. Lett.* **59**, 2935 (1987).
 - [3] J. Hoffnagle, R. G. DeVoe, L. Reyna, and R. G. Brewer, *Phys. Rev. Lett.* **61**, 255 (1988).
 - [4] R. G. Brewer, J. Hoffnagle, and R. G. DeVoe, *Phys. Rev. Lett.* **65**, 2619 (1990).
 - [5] R. G. Brewer, J. Hoffnagle, R. G. DeVoe, L. Reyna, and W. Henshaw, *Nature (London)* **344**, 305 (1990).
 - [6] P. Bak, *Phys. Today* **39**, No. 12, 39 (1986).
 - [7] R. Blümel, C. Kappler, W. Quint, and H. Walther, *Phys. Rev. A* **40**, 808 (1989).
 - [8] R. F. Wuerker, H. Shelton, and R. V. Langmuir, *J. Appl. Phys.* **30**, 342 (1959).
 - [9] W. Neuhauser, M. Hohenstatt, P. Toschek, and H. Dehmelt, *Phys. Rev. Lett.* **41**, 233 (1978).
 - [10] R. G. DeVoe, J. A. Hoffnagle, and R. G. Brewer, *Phys. Rev. A* **39**, 4362 (1989).
 - [11] T. Sauter, H. Gilhaus, I. Siemers, R. Blatt, W. Neuhauser, and P. E. Toschek, *Z. Phys. D* **10**, 153 (1988).
 - [12] J. P. Gordon and A. Ashkin, *Phys. Rev. A* **21**, 1606 (1980).
 - [13] W. M. Itano and D. J. Wineland, *Phys. Rev. A* **25**, 35 (1982).
 - [14] S. Stenholm, *Rev. Mod. Phys.* **58**, 699 (1986).
 - [15] M. Abramowitz and I. A. Stegun, *Handbook of Mathematical Functions* (U.S. GPO, Washington, DC, 1968).
 - [16] N. H. Press, B. P. Flannery, S. A. Teukolsky, and W. T. Vetterling, *Numerical Recipes* (Cambridge Univ. Press, Cambridge, 1987).
 - [17] J. A. Yorke, *Dynamics* (Univ. of Maryland, College Park, 1990).
 - [18] M. H. Jensen, P. Bak, and T. Bohr, *Phys. Rev. A* **30**, 1960 (1984); **30**, 1970 (1984).

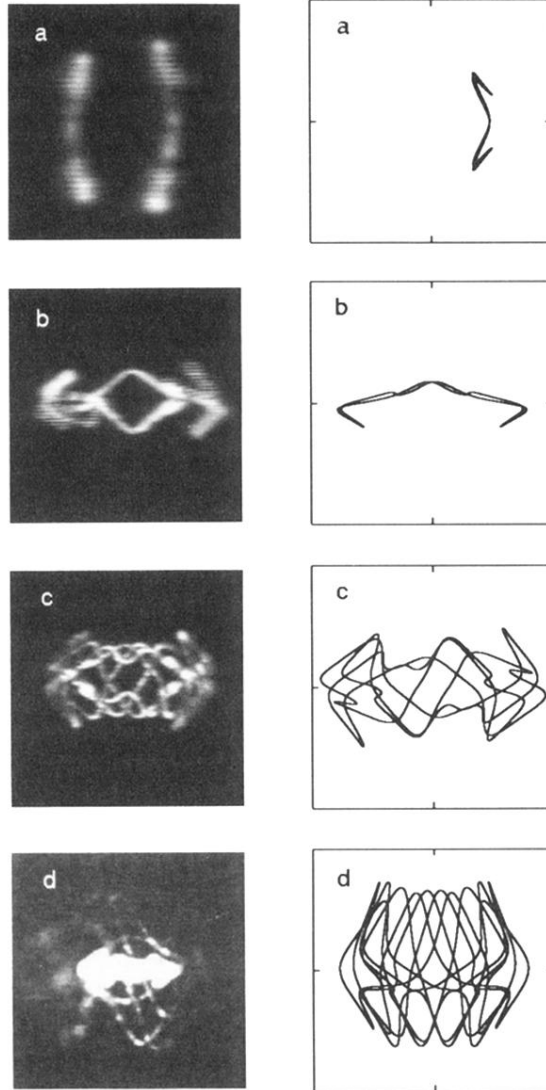


FIG. 1. Frequency-locked two-particle Coulomb clusters. Left column: photographs taken with cw illumination. Right column: computed trajectories of the relative coordinate (r, z) of the two particles for the same q values and $\Gamma = 10^{-2}$. The values of q and winding numbers (w_r, w_z) are (a): $q = 0.72$, $(4/4, 1/4)$; (b): $q = 0.74$, $(1/8, 2/8)$; (c): $q = 0.78$, $(3/22, 7/22)$; and (d): $q = 0.79$, $(5/36, 12/36)$. The mass ratio of the particles is approximately 1 in (a)–(c) and 1.25 in (d).